Reprinted from:

THE JOURNAL OF CHEMICAL PHYSICS VOLUME 55, NUMBER 3 1 AUGUST 1971

Thermodynamic Properties of the Fluid and Solid Phases for Inverse Power Potentials*

WILLIAM G. HOOVER, STEVEN G. GRAY, AND KEITH W. JOHNSON

Lawrence Radiation Laboratory, University of California, Livermore, California 94550

(Received 18 March 1971)

The two computer methods of Monte Carlo and lattice dynamics are used to determine fluid and face-centered-cubic solid thermodynamic properties for classical particles interacting with pairwise-additive inverse 4th, 6th, and 9th power potentials. These results, together with those already on hand for 12th power and hard-sphere potentials, provide a complete, and remarkably simple, description of the dependence of the pure-phase thermodynamics and the melting transition on the "softness" of the pair potential.

I. INTRODUCTION

Except for the simplest materials there have been few attempts to calculate thermodynamic properties directly from actual intermolecular forces. Such forces can be obtained only by solving a complicated many-electron problem which is still challenging for even the two simplest cases, molecular hydrogen[1] and helium.[2] For more complicated systems uncertainty in the pair interactions coupled with uncertainty and practical difficulty in estimating and calculating many-body forces precludes accurate first-principles thermodynamic calculations in the near future.[3]

In view of these mathematical difficulties most people find it more rewarding and enlightening to carry out calculations based on well-defined microscopic *models* (where the forces are *prescribed* rather than calculated) and to compare the results for the model with experiment. An important goal of these calculations is to find out what qualitative features of the models are crucial for particular kinds of thermodynamic or hydrodynamic behavior. We already know, from the hard-sphere calculations,[4,5] that at high pressure strong repulsive forces are sufficient for the existence of a solid phase; the present work shows that even the soft forces from a weak r^{-4} repulsive potential are strong enough to stabilize a solid. It seems likely that for molecules with central forces, attractions are necessary for two different fluid phases to coexist. The details of the effect of the forces on the phase diagram are not well understood; even less well understood are the more complicated features in phase diagrams such as melting point maxima (at which $dT_{\text{melt}}/dP_{\text{melt}}$ vanishes), rotational, and insulator-to-metal transitions.

Here we study the dependence of thermodynamic behavior on the "softness" of the forces; soft forces are those which change slowly and gradually as the distance between particles is varied. We relate the microscopic "softness" of the particles to the macroscopic compressibility and phase boundaries of the solid and the fluid. Since the simplest possible model consistent with the facts should be used, we here study the *simplest* family of pair potentials. The simplicity results in a unique property: a single isotherm, isochore, or isobar is sufficient to determine the entire phase diagram. This family of pair potentials is the set of inverse powers:

$$\phi(r) = \epsilon(\sigma/r)^n. \tag{1}$$

Potential functions corresponding to representative values of n are shown in Fig. 1.

The simplicity of the thermodynamic and hydrodynamic properties of these inverse power potentials has not gone unrecognized.[6,7] The earliest correct kinetic theory calculations showed that the scattering cross section at fixed density varies with temperature exactly as $T^{-2/n}$ and the collision rate as $T^{(n-4)/2n}$ for the nth power repulsion. The hard-sphere case ($n=\infty$), with constant cross section, and the Maxwellian case ($n=4$), with constant collision rate, were the simplest cases and therefore the most extensively studied. Neither of these choices is particularly "realistic" because they both lie outside the normal range of n used in reproducing experimental data (roughly from 6 to 12). Although the $n=5$ repulsion is quite soft, the distribution functions for that potential are of relatively recent special interest because they provide an approximate description of the molecular distribution in ground-state helium.[8,9]

The special simplicity of the inverse power potential can be seen in several ways. First, note that no conceivable experiment could determine separately the ϵ and the σ which appear in the interaction energy of Eq. (1) because only the *combination* $\epsilon\sigma^n$ contributes to the energy or to forces derived from that energy. Second, from the viewpoint of molecular dynamics, characteristic time and distance scales $[(kT/m)^{1/2}$ and $(V/N)^{1/3}]$ can be introduced to show that the detailed dynamic evolution for systems with identical scaled initial conditions and with the same value of $(N\sigma^3/V)\,(\epsilon/kT)^{3/n}$ are identical. This remarkable simplification of the dynamic behavior occurs only for the inverse power potentials. Finally, from the viewpoint of statistical mechanics, the canonical partition function shows that the nonideal part of the Helmholtz free energy depends only on the dimensionless combination $(N\sigma^3/V)\,(\epsilon/kT)^{3/n}$. All three viewpoints show that a single variable combining the energy and distance scales can describe the whole range of thermodynamic states.

The classical virial theorem giving the pressure in terms of the forces on the particles is also simplified for

inverse powers because the forces and the pressure can be related directly to the energy. This virial relation shows that, apart from a multiplicative factor of $s=3/n$ (the softness), $0\leq s\leq 1$, the excess energy density $(E-\frac{3}{2}NkT)/V$ and excess pressure $(PV-NkT)/V$ are given by the *same* microscopic expressions:

$$\Phi/NkT=(E-\tfrac{3}{2}NkT)/NkT$$
$$=\left\langle\sum\frac{\epsilon(\sigma/r)^n}{NkT}\right\rangle$$
$$=(3/n)[(PV-NkT)/NkT]. \qquad (2)$$

"Excess" properties are measured with respect to an ideal gas at the same V and T. With $P(V)$ or $E(T)$ computed, the excess Helmholtz free energy A^e can then be determined by either an excess pressure P^e or excess energy E^e integration:

$$\frac{A^e}{NkT}=\int_V^\infty\frac{P^eV}{NkT}\frac{dV}{V}=\int_T^\infty\frac{E^e}{NkT}\frac{dT}{T}. \qquad (3)$$

If the virial relation (2) is taken into account it is easy to show that the two integrals in (3) are identical.

In this paper we calculate the thermodynamic properties using the Monte Carlo and lattice dynamics methods. We then present the results for the fluid and (face-centered) solid phases in a systematic way so that the thermodynamic state, pressure, and energy can be calculated for *any* inverse power directly. We plan a more detailed study of the solid portion of the phase diagram in the future.

For guidance in proceeding from these simple models to more complicated ones we study the usefulness of several approximations (the virial series, hard-sphere perturbation theory, and lattice dynamics) as a function of the softness, $s=3/n$.

II. NUMERICAL METHODS AND THEIR LIMITATIONS

A. Monte Carlo

Metropolis, Rosenbluth,[2] and Teller[2] first applied the "Monte Carlo" method to statistical mechanics.[10,11] They pointed out that a simple scheme for selecting among random particle moves [allowing all moves which lower the potential energy Φ of the system but prohibiting a fraction $1-\exp(-\delta\Phi/kT)$ of moves raising that energy by $\delta\Phi$] eventually produces the same averages as an exact evaluation of the corresponding partition function. Both fluids and solids can be treated by Monte Carlo. The only catch in this method is that in practice available computing time limits the accuracy of the results.

The Monte Carlo method is ideal for two- or three-digit accuracy (which is far more accurate than the results from approximate theories, except in very special circumstances). Results obtained using it have been compared with those from the alternative "molecular dynamics" method in which the time history of a system is followed. The two methods agree closely, even for relatively small systems, and are fast enough so that it is now practical to determine an entire phase diagram (gas, liquid, and solid) for a realistic potential.[12]

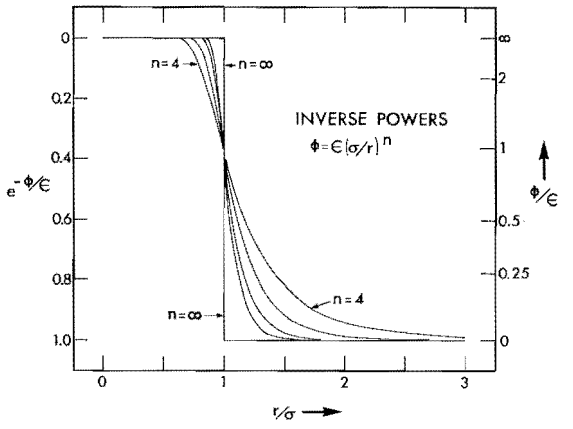

FIG. 1. Interparticle potential energy functions for the five inverse power potentials, $n=4$, 6, 9, 12, and ∞.

Both the Monte Carlo method, which we use here, and the molecular dynamics method have become accepted by most workers in the field as reliable sources for accurate "experimental" data. Those less familiar with these two numerical "brute-force" methods are characteristically suspicious that the relatively small number of particles treated (10^3 relative to 10^{23}) can somehow lead to large errors. Actually, except near phase boundaries or with very long-range forces, the errors in the numerical methods are small. Careful study of the computer results has shown that the typical errors, provided periodic boundaries are used to eliminate surface effects, are of order $1/N$ or $\ln N/N$ (where N is the number of particles) in the intensive properties. This mild number dependence can be predicted theoretically in the limiting cases of low[13] or high[14] density. For long-range potentials ($n<6$) the "truncation error" due to cutting off the range of the pair potential dominates. This introduces an error of order $N^{(3-n)/3}$. The error can be avoided by using Ewald's method to evaluate potential energy sums for an infinite periodic array rather than a finite one.[15]

The uncertainty of Monte Carlo results is generally estimated from the fluctuations in the numerical data. Such fluctuations would not be able to reveal systematic errors in the results, but recent work using a new method has shown[16] that no significant errors exist. This method is based on "single-occupancy" calculations in which each particle is restricted to lie within its own individual cell. Throughout the range of solid-phase densities the restrictions imposed by the cell walls are numerically unimportant, and the single-occupancy system faithfully behaves like an ordinary solid.[16,17] At high enough compression this solid's free energy

can be calculated exactly, using lattice dynamics. The very low-density free energy for the single-occupancy system can also be calculated, because it corresponds to that of N independent ideal-gas particles. Then the known free energy difference between these two limits can be used to check the accuracy of the computer-generated pressures, because the free energy difference ΔA^e must agree with the pressure integral $-\int P^e dV$. This numerical check of the Monte Carlo isotherm shows that within the uncertainty imposed by statistical fluctuations there are no errors in the results as large as the expected $1/N$ and $\ln N/N$ terms.

B. Lattice Dynamics

The lattice dynamics method for calculating thermodynamic properties is based on expanding the potential energy Φ as a power series in the particle displacements (relative to the center of mass) and then truncating the series after the quadratic terms.[18] The resulting partition function then factors into a product of "normal-mode" partition functions, $kT/h\nu_i$, for the ith mode:

$$\exp\left(-\frac{A_{LD}}{kT}\right)=\exp\left(-\frac{\Phi_0}{kT}\right)\left(\frac{V}{N}\right)\left(\frac{2\pi NmkT}{h^2}\right)^{3/2}\prod_{i=1}^{3N-3}\frac{kT}{h\nu_i}. \tag{4}$$

The terms multiplying the product are the contributions of the center of mass and the static-lattice potential energy Φ_0. At high density (or low temperature) the rms vibration amplitude goes to zero as $V^{(n+2)/6}$ (or $T^{1/2}$) so that the small-vibration basis of lattice dynamics becomes exactly correct. The lattice dynamics free energy calculation can be carried out very precisely with nearly the number of significant figures carried by the computing machine and so in this high density limit is more accurate than the Monte Carlo free energy.

Besides furnishing a useful check on the single-occupancy pressure integration, lattice dynamics can also be used to determine solid-phase thermodynamic properties and their number dependence.[14,19] In applying lattice dynamics to number-dependent properties, it is obviously essential to calculate the discrete set of $3N-3$ frequencies at which the periodic N-particle system can vibrate. [For an N particle one-dimensional crystal the frequencies to be calculated correspond to wavelengths which would fit inside the periodic box, L, $L/2$, $L/3$, $\cdots L/(N-1)$ for a box of length L; the L/N case corresponds to center of mass motion and has to be treated separately.] The conventional treatment samples instead frequencies from the continuous distribution appropriate to an infinite crystal.

Despite its long history of 60 years and a huge descriptive literature, lattice dynamics is still relatively inaccessible for nonexperts interested in applying the method to numerical problems. The inaccessibility is mostly due to semantic difficulties. Such innocent phrases as "harmonic approximation" and "central forces" have several different interpretations. In our own "lattice dynamics" calculations we expand the potential energy *at the density of interest* so that the expansion coefficients depend on density and include contributions from both the first and second derivatives of the pair potential ϕ. The expansion coefficients are given by Eqs. (29.3) and (29.4) of Ref. 18. We then solve Eqs. (24.7) and (24.8) for the vibration frequencies. For inverse power potentials only a single density has to be studied because all frequencies depend on density in a simple way, $\nu_i \propto V^{-(n+2)/6}$. For other potentials, incidentally, the simplest route to thermodynamics from lattice dynamics is through *numerical* differentiation of the free energy.[19] The pressure and the coefficients describing the work necessary to distort a crystal (elastic constants) can be obtained with four-figure accuracy by fitting a polynomial to several free energies calculated for closely spaced distortions. This procedure is much simpler than the more "natural" approach of expanding the equations of lattice dynamics about the undistorted state.

By using the numerical method, thermodynamic properties can be calculated with a computer program of only 50 cards plus an eigenvalue subroutine. The one tricky point arises in setting up the "dynamical matrix" for a finite crystal. The potential energy convention used in the Monte Carlo work is Wood's "nearest-image" convention in which the distance between Particles i and j used in calculating the energy is based on the nearest of any periodic images of j (generated by repeating the N particle system periodically to fill all space) that happens to lie closer to i than does j itself. In lattice dynamics the potential is expanded about the perfect lattice configuration. In a "perfect lattice" there are, typically, many pairs of particles separated by *exactly* half the box length in one or more of the three coordinate directions so that there is no unique "closest" j. In setting up the dynamical matrix any pair separated by half the box length in the x direction should be entered into the matrix twice (both times with weight $\frac{1}{2}$), once with an x separation of $\frac{1}{2}L$ and once with $-\frac{1}{2}L$. A pair of particles separated by $(\frac{1}{2}L, \frac{1}{2}L, \frac{1}{2}L)$ in the perfect crystal would contribute $8(=2\times2\times2)$ times to the matrix.

For forces of short enough range that $\phi'(\frac{1}{2}L)$ and $\phi''(\frac{1}{2}L)$ are negligible, the lattice dynamics and Monte Carlo free energies agree at high density. If these derivatives are not negligible, then the nearest-image convention leads to difficulties in the Monte Carlo work. Two particles initially separated by $\frac{1}{2}L$ in the x direction can only get closer to each other under the nearest-image convention. Thus the potential energy contains a contribution of the form $\phi(\frac{1}{2}L-|\delta x_i-\delta x_j|)$, where δx_i and δx_j represent displacements from perfect-crystal locations. Such a term destroys the validity of the low-temperature expansion of thermodynamic properties in powers of temperature, and in practice makes it necessary to use the Ewald method for greater accuracy. In retrospect, we should have used that method for our inverse 4th power calculations.

III. RESULTS

Most of the past computer studies have focused on PV isotherms rather than on isochores or isobars. There are two reasons for this emphasis. First, the pressure-volume equation of state is more often measured in the laboratory. Second, the pioneering calculations of Alder, Wainwright, and Wood[4] were based on the hard-sphere potential which has no excess potential energy to study. The average potential energies measured in our Monte Carlo work are given in Tables I–III for the inverse 4th, 6th, and 9th powers. Because we were especially interested in locating the fluid–solid phase transition we measured the energy of the fluid phase and the single-occupancy solid phase from zero density up to the transition density. The free energy of the zero-density fluid lies below that of the zero-density single-occupancy "solid" (with particles confined to spherical cells) by $1.3005NkT$. The transition is then located, just as in the inverse 12th power case,[16] by integrating to the density at which the free energies of the two phases match. The melting and freezing densities could be located within 1% or 2% from the relatively crude data of Tables I–III. In the inverse 4th power Maxwellian molecule case the uncertainty is greater (probably 5%) because the results depend so strongly on the number of particles.

The melting characteristics of the inverse power potentials are given in Table IV and plotted, as functions of the softness of the potential, in Fig. 2. Two approximate melting rules, Lindemann's and Ross', agree well with the data. The older rule is Lindemann's, which states that the root-mean-squared displacement of particles from their lattice sites is a universal fraction, f, of the nearest-neighbor spacing at melting. Although the law breaks down qualitatively for two-dimensional crystals (rms displacement is infinite in the thermodynamic limit for such crystals[20]) it is empirically well justified for simple metals.[21] The Lindemann fraction f is itself hard to measure in computer experiments. Center-of-mass motion artificially increases the displacement[22] while the small system size artificially decreases it (by an amount of order $N^{-1/3}$, several percent for a few hundred particles). To test the Lindemann relation we have used the lattice dynamics approximation:

$$f^2 \equiv \langle r^2 \rangle / d^2 \doteq (3kT/md^2)\langle \omega^{-2} \rangle. \tag{5}$$

This approximation is *exact* if anharmonic (cubic, quartic, $\cdots$) terms in the particle displacements can be ignored.[23] Just how important the anharmonic terms are at melting can only be determined by long computer calculations. Most calculations carried out so far are either approximate[21] or of uncertain accuracy at melting.[24] The values we get from lattice dynamics are all quite close to 0.15. There is a small systematic variation with softness in Fig. 2. Hansen studied the variation of f with temperature along the melting line for the Lennard-Jones potential.[17] His results change very little with temperature (from 0.15 to 0.14). For hard spheres Young and Alder have carefully measured the Lindemann fraction at melting. They used a fixed center of mass (molecular dynamics with periodic

TABLE I. Potential energy increase over the static lattice energy for inverse 4th power particles (Maxwellian molecules). $(\Phi-\Phi_0)/NkT$ is tabulated for periodic systems of 32, 108, and 256 particles. The solid data are all for single-occupancy systems in which each particle is confined to a spherical cell with diameter equal to the face-centered-cubic nearest-neighbor spacing. Φ_0/NkT is 7.1493, 9.0977, 10.0194, and 12.66915 times $\rho^{4/3}\epsilon/kT$ for 32, 108, 256, and ∞ particles. The combination $(N\sigma^3)/(\sqrt{2}V)$ is ρ. The number of accepted moves was approximately 100 000. The statistical fluctuations in most of the results suggest errors of order 1% or less.

	Fluid			Solid		
$\rho(\epsilon/kT)^{3/4}$	32	108	256	32	108	256
0.10	0.335	0.330	0.331	0.224	0.213	0.210
0.25	0.631	0.607	0.605	0.493	0.455	0.453
0.50	1.001	0.929	0.907	0.844	0.771	0.755
1.00	1.595	1.393	1.347	1.403	1.206	1.173
1.50	2.083	1.719	1.644	1.834	1.531	1.468
2.00	2.536	2.022	1.887	1.896	1.786	1.686
2.50	2.97(f)[a]	2.276	2.055	1.906	1.831	1.808
3.00		2.518	2.262	1.909	1.824	1.739
3.50		2.635	2.412			
4.00		2.872	2.583	1.967		

[a] (f) indicates that this system froze, ending up in the face-centered-cubic structure. The quoted energy was obtained from the plateau observed prior to freezing.

TABLE II. Potential energy increase over the static lattice energy for inverse 6th power particles. $(\Phi-\Phi_0)/NkT$ is tabulated for periodic systems of 32, 108, and 256 particles. The solid data are all for single-occupancy systems in which each particle is confined to a spherical cell with diameter equal to the face-centered-cubic nearest-neighbor spacing. Φ_0/NkT is 6.4355, 7.0190, 7.1432, and 7.2270 times $\rho^2\epsilon/kT$ for 32, 108, 256, and ∞ particles. The combination $(N\sigma^6)/(\sqrt{2}V)$ is ρ. The number of accepted moves was approximately 100 000. The statistical fluctuations in most of the results suggest errors of order 1% or less.

	Fluid			Solid		
$\rho(\epsilon/kT)^{1/2}$	32	108	256	32	108	256
0.10	0.244	0.248	0.247	0.156	0.152	0.152
0.25	0.575	0.569	0.577	0.444	0.445	0.438
0.50	1.057	0.996	1.036	0.921	0.888	0.879
1.00	1.904	1.744	1.739	1.658	1.559	1.529
1.50	2.626	2.218	2.195	1.566	1.555	1.569
2.00	(f)[a]	2.428(g)[b]		1.637	1.519	1.533
2.50				1.657	1.544	1.503
3.00				1.705	1.526	1.533

[a] (f) means this system froze in a face-centered-cubic arrangement before a plateau for the fluid pressure could be established.

[b] (g) the slowness with which the pressure decreased suggests a glassy state intermediate between the fluid and solid branches.

TABLE III. Potential energy increase over the static lattice energy for inverse 9th power particles. $(\Phi-\Phi_0)/NkT$ is tabulated for periodic systems of 32, 108, and 256 particles. The solid data are all for single-occupancy systems in which each particle is confined to a spherical cell with diameter equal to the face-centered-cubic nearest-neighbor spacing. Φ_0/NkT is 6.1121, 6.2374, 6.2449, and 6.2463 times $\rho^3\epsilon/kT$ for 32, 108, 256, and ∞ particles. The combination $(N\sigma^3)/(\sqrt{2}V)$ is ρ. The number of accepted moves was approximately 100 000. The statistical fluctuations in most of the results suggest errors of order 1% or less.

	Fluid			Solid		
$\rho(\epsilon/kT)^{1/3}$	32	108	256	32	108	256
0.10	0.153	0.158	0.159	0.092	0.093	0.091
0.25	0.463	0.467	0.469	0.358	0.363	0.359
0.50	1.081	1.088	1.086	0.948	0.939	0.937
1.00	2.269	2.143	2.199	1.413	1.443	1.451
1.50	3.987	(g)	(g)	1.470	1.457	1.456
2.00	(g)[a]			1.488	1.484	1.491
2.50				1.545	1.463	1.513
3.00				1.552	1.503	1.485

[a] (g) means these systems did not reach equilibrium. The 32-particle fluid became stuck in a glassy configuration; the larger systems slowly decreased in energy throughout the runs at $\rho(\epsilon/kT)^{1/3}=1.50$.

boundaries) and extrapolated their small-system results to the thermodynamic limit, finding[25] f(hard spheres) = 0.126. It seems possible that the hard-sphere value is somewhat anomalous due to the extreme anharmonicity of that crystal. The Lindemann parameter may undergo a change for n so large that the solid phase becomes hard-sphere-like before melting.

Ross' approximate melting rule was proposed in 1969 in the context of the cell model.[26] Ross suggested that the thermal part of the excess Helmholtz free energy $(A^e-\Phi_0)/NkT$ is constant along the melting line. In pictorial terms the free volume is a characteristic fraction of the volume per particle at melting. This rule closely resembles Lindemann's and, like Lindemann's, is exact for any particular inverse power potential.[27] The question is whether or not the constant is the same for a whole set of potentials. Our inverse power results

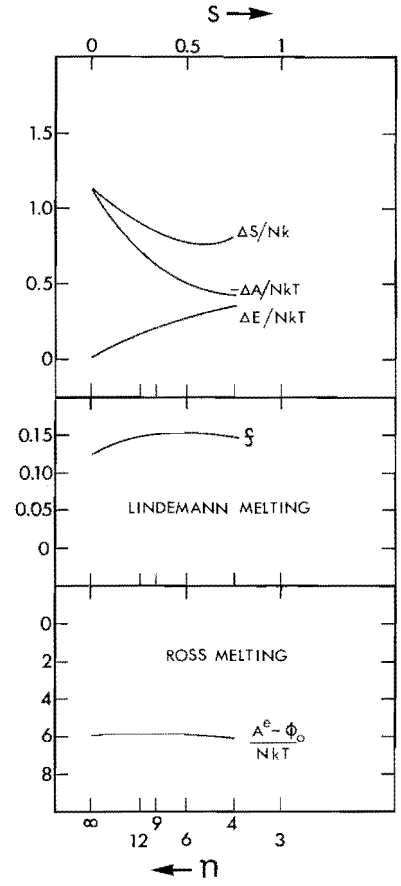

FIG. 2. Melting (at constant temperature and pressure) parameters as functions of softness, $s=3/n$. The thermodynamic differences in the top part of the figure are taken in the sense fluid property minus solid property. The Lindemann melting rule test in the center of the figure is approximate, except for the hard-sphere case ($s=0$). The other values of the Lindemann function f, rms displacement divided by nearest-neighbor spacing, were calculated using lattice dynamics. The hard-sphere value was supplied by David Young. Ross' melting rule, tested at the base of the figure, states that the thermal excess Helmholtz free energy (which can be related to a reduced free volume) is proportional to the temperature. The figure indicates a proportionality constant $+6Nk$.

TABLE IV. Melting characteristics of the inverse power potentials. The freezing and melting conditions together with the free energy, potential energy, and entropy changes for melting (at constant pressure and temperature) are tabulated. All the differences (Δ) are given in the sense fluid minus solid. The inverse 12th power properties come from Refs. 16 and 17. The hard-sphere melting properties come from Ref. 28. For hard spheres ρ is the ratio of the density to the density at close packing. For all the inverse powers we use the same definition, $\rho\equiv(N\sigma^3)/(\sqrt{2}V)$. Similarly, V_0 stands for $N\sigma^3/\sqrt{2}$. The uncertainty in the melting pressure is about 5% for the 4th, 6th, and 9th power potentials and about half that for the 12th power and hard-sphere potentials. The uncertainty in the fusion entropy ranges from about $0.2Nk$ ($n=4$) to about $0.1Nk$ (hard spheres).

	$n=4$	$n=6$	$n=9$	$n=12$	$n=\infty$
$\rho(\epsilon/kT)_{\text{melt}}^{3/n}$	3.94	1.56	0.971	0.844	0.736
$\rho(\epsilon/kT)_{\text{freeze}}^{3/n}$	3.92	1.54	0.943	0.813	0.667
$\Delta A/NkT$	−0.45	−0.50	−0.63	−0.72	−1.16
$\Delta E/NkT$	0.35	0.25	0.21	0.18	0.00
$\Delta S/Nk$	0.80	0.75	0.84	0.90	1.16
PV_0/NkT	426	61	22	16	8.3

together with the older data for the inverse 12th power and for hard spheres show that the excess Helmholtz free energy is approximately $+6NkT$ in all these cases. The extreme value 6.3 for the inverse fourth power potential is apparently significantly higher than the rest, but it is conceivable that the extreme number dependence of the 4th power results is responsible for this disparity. Except for the very soft $n=4$ case, Ross' melting rule, with an excess free energy of $6NkT$,

satisfies the data. This insensitivity of this free energy to the forces suggests that Ross' rule will be generally useful. The variation of the thermal Helmholtz free energy with softness is much less than the variation in the thermal energy or the thermal entropy. Ross' melting rule *can* be applied to two-dimensional systems. For hard disks the excess free energy at melting is $3.9NkT$.[28]

Our pressure–volume isotherms (with the perfect-lattice and ideal-gas contributions subtracted) are plotted in Fig. 3. Also included are the hard-sphere[28] and inverse 12th power[16,17] isotherms. The data, covering a range of softness from 0 to $\frac{3}{4}$, show little apparent regularity.

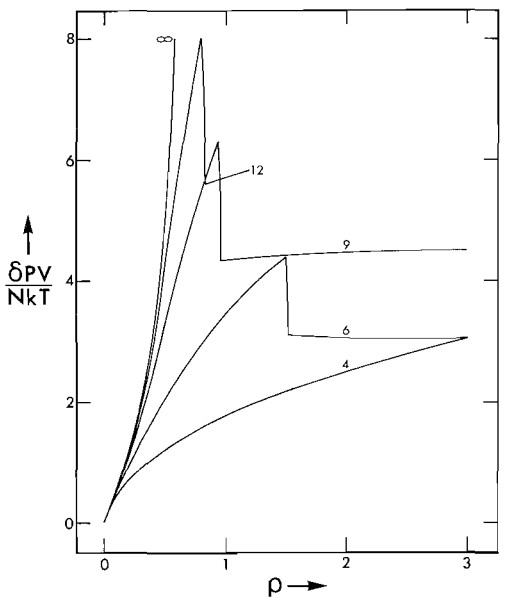

FIG. 3. The thermal excess compressibility factor $(P-P_{\text{static}}-P_{\text{ideal}})V/NkT$ along the isotherm $\epsilon\equiv kT$. The ratio of the density to the close-packed (for hard spheres) density, $(N\sigma^3)/(\sqrt{2}V)$ is ρ. The maxima in the curves correspond to freezing. A nearly vertical portion connects the freezing and melting densities.

In an effort to present our results in a more systematic way we decided to exploit the high-density low-temperature harmonic limit. In this limit *any* inverse power potential has an excess energy of $3NkT$ over the static perfect-lattice value. This suggests that $E(T)$ rather than $P(V)$ deserves study. Of course pressure can still be obtained from energy using the virial theorem, Eq. (2). The energy–temperature isochores are shown in Fig. 4. In that figure there *is* a regular variation with softness. All four curves have about the same shape with the softer crystals melting at lower temperatures. Interestingly enough, the Brush, Sahlin, and Teller results for the inverse *first* power potential[29] (a one-component Coulomb system with a uniform neutralizing background charge) have a similar shape.

Although the energy–temperature isochores of Fig. 4 are adequate for interpolation purposes, it is desirable

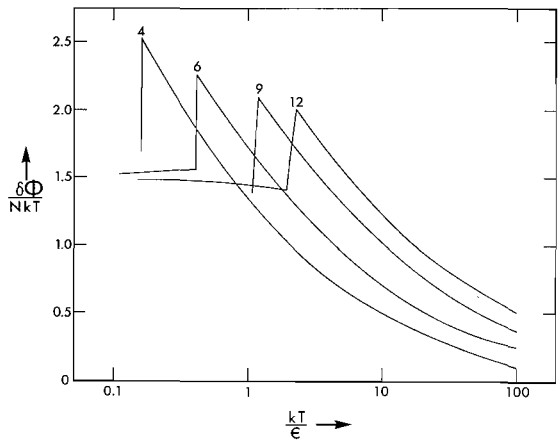

FIG. 4. The thermal excess energy $(E-E_{\text{static}}-E_{\text{ideal}})/NkT=(\Phi-\Phi_{\text{static}})/NkT$ for inverse power potentials along the isochore $\rho\equiv 1$. The zero-temperature limit for the reduced energy is 1.5. The maxima correspond to the freezing temperatures.

to identify the offset between the curves as a function of softness. Although the solid-phase Lindemann relation produces a suitable temperature scale for locating the melting breakpoint, this same scaling does not give good correspondence for the fluid phase energies. Resulting errors in the thermal energy would be as large as 20%. Alternative temperature scales could be based on any moment of the frequency distribution function. The most natural one is the Einstein frequency[30] ν_E, the frequency at which a single particle would vibrate if all the others in the crystal were held fixed at their lattice sites. This same frequency is also the second moment of the lattice dynamics frequencies: $(1/3N)\sum\nu^2\equiv\nu_E^2$. A temperature scale based on the Einstein frequency turns out to correlate the fluid thermodynamics very well. This is illustrated by Fig. 5, where the thermal potential energy $(\Phi-\Phi_0)$ is plotted as a function of the Einstein approximation to $\langle r^2\rangle/d^2$, namely $3kT/m(2\pi\nu_E d)^2$. All the data lie on nearly the

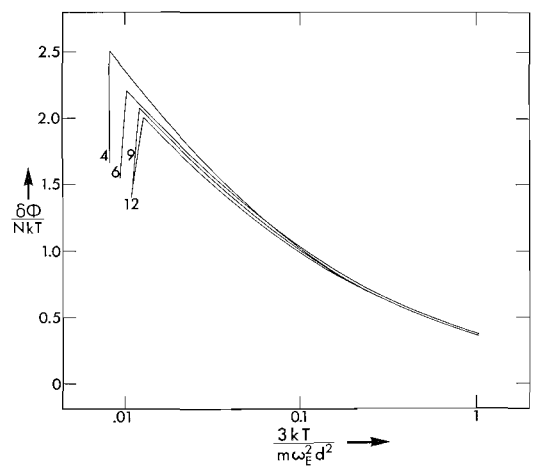

FIG. 5. The thermal excess energy $(\Phi-\Phi_{\text{static}})/NkT$ as a function of the harmonic Einstein approximation to $\langle r^2\rangle/d^2$. The maxima correspond to the freezing points.

TABLE V. Second and third virial coefficients for inverse power potentials. Barker, Leonard, and Pompe [J. Chem. Phys. **44**, 4206 (1966)] describe efficient methods for calculating the first five coefficients in the expansion $PV/NkT=1+B_2(N/V)+B_3(N/V)^2+\cdots$.

	$n=4$	$n=6$	$n=9$	$n=12$	$n=\infty$
$B_2(kT/\epsilon)^{3/n}(\sqrt{2}/\sigma^3)$	10.7388	5.2499	4.0108	3.6296	2.9619
$B_3(kT/\epsilon)^{6/n}(\sqrt{2}/\sigma^3)^2$	18.1018	11.1040	8.5513	7.5821	5.4831

same universal curve. There are small systematic trends: the softer potentials have slightly higher energies and slightly lower melting temperatures. The over-all simplicity of the results is striking.

With the universal equation of state shown in Fig. 5, our effort to systematize the inverse-power equations of state is complete. For any potential one can calculate the Einstein frequency and then use a Grüneisen theory[31] to relate the thermal energy to the thermal pressure. A theory *predicting* the curve shown in Fig. 5 is desirable. We have no such theory. The data can be represented by the form

$$(\langle r^2\rangle/d^2)_E=A\,\exp[-B(\delta\Phi/NkT)^c],$$

with $A=1900$, $B=9.8$, and $c=0.26$.

IV. APPROXIMATIONS

With our results in hand we can consider the usefulness of approximations which could be applied to more complicated force laws. At low density the virial expansion of pressure in powers of the density is exact.[32] For the inverse powers the same series provides an expansion of the energy in fractional powers of the temperature. The second and third virial coefficients, B_2 and B_3 in the expansion $PV/NkT=1+B_2(N/V)+B_3(N/V)^2+\cdots$ appear in Table V. Although the table shows that $B_3/(B_2)^2$ decreases with increasing softness, we found empirically that the virial series becomes less useful as the potential softens. Two effects are responsible. First, the freezing transition moves to higher and higher density; second, the mean-field contribution to the pressure dominates over the effect of isolated few-particle collisions as the potential becomes soft. Just how the virial series, a series in $1/V$, accounts for a mean field of order $V^{-n/3}$ is not clear. In the Maxwellian molecule case 95% of the pressure at freezing comes from the static perfect-lattice contribution. The thermal pressure is a small perturbation.

In the exploratory stages of this work we found the Mansoori–Canfield hard-sphere perturbation theory to be a useful approximate guide to fluid-phase thermodynamics. This theory[33] uses a hard-sphere diameter which is varied to produce the lowest possible Helmholtz free energy (in the approximation of first-order perturbation theory). The resulting free energy is then numerically differentiated to get thermodynamic properties. Convenient approximations to the hard-sphere pair distribution function and to the hard-sphere free energy simplify this calculation. We found that the perturbation theory results for the energy were invariably too high (by amounts of order 0.1 to $0.2NkT$ in the dense fluid range), but the smooth curves produced by this theory were useful guides for interpolation between the widely spaced Monte Carlo data points. Of course, once Fig. 5 had been constructed, the perturbation theory was no longer necessary.

In the solid phase the simplest approximation is the Einstein approximation in which a single particle moves in the field of its neighbors. At low temperatures only the quadratic term in the field contributes to thermal properties and the resulting one-particle approximation to the Helmholtz free energy can be compared with the (exact) low-temperature lattice dynamics result:

$$\frac{(A_E-A)}{NkT}=N^{-1}\sum^{3N-3}\ln\left(\frac{\nu_E}{\nu}\right)\equiv C(N). \qquad (6)$$

Numerical results for small periodic crystals and for the thermodynamic limit are given in Table VI. The Einstein model free energy is uniformly higher than the lattice dynamics free energy. The error increases from $0.24689NkT$ to $0.51266NkT$ as the softness increases from 0 to 0.75. The free energies from lattice dynamics were verified (within about $0.08NkT$) by numerical integration of our single-occupancy data between the low- and high-density limits. The discrepancies found were no larger than would be expected from the Monte Carlo statistical fluctuations.

The ratio of the mean-squared displacement from lattice dynamics to the one-particle approximation is also given in Table VI. Here the errors are greater, nearly a factor of 3 for the Maxwellian particles.

In the present work we have not made an accurate estimate of anharmonic solid properties. For that rather long computer runs would be required. Results so far available[34] indicate that the straightforward first-order perturbation approach does not converge well near melting. The full perturbation theory would give energy as a power series in T (or equivalently pressure as a series in fractional powers of the volume). A quantitative investigation of the convergence would certainly be of interest.

V. CONCLUDING REMARKS

It is especially interesting that the macroscopic properties of the inverse power fluid and solid can be

TABLE VI. Properties for inverse power potentials in the face-centered-cubic solid phase. Periodic boundaries and the nearest-image potential convention are used. The Einstein frequency, $\nu(\text{Einstein}) \equiv \omega(\text{Einstein})/(2\pi)$, is the frequency at which a single particle would vibrate if the others were held fixed in their perfect lattice positions. The reduced density, ρ, is $(N\sigma^3)/(\sqrt{2}V)$. The ratio $\langle[\nu(\text{Einstein})/\nu]^2\rangle$ is the ratio of the mean squared displacement (in the lattice dynamics approximation) to that predicted by the Einstein approximation, $3kT/[m\omega^2(\text{Einstein})]$. The coefficient $C(N)$ defined in Eq. (6) of the text gives a quantitative comparison between the Helmholtz free energy (with center of mass fixed) according to lattice dynamics and the Helmholtz free energy according to the Einstein model, $[A(\text{Einstein}) - A(\text{Lattice Dynamics})]/NkT \equiv C(N)$.

A. Einstein frequencies. $\nu(\text{Einstein})\sigma(m/\epsilon)^{1/2}\rho^{-(n+2)/6}$ for $n=4$, 6, 9, and 12. These frequencies apply to face-centered-cubic periodic crystal in which the central particle interacts with $N-1$ neighbors.

N	$n=4$	$n=6$	$n=9$	$n=12$
4	0.5513	0.8717	1.3505	1.8286
32	1.1420	1.7686	2.7118	3.6615
108	1.1926	1.7974	2.7232	3.6661
256	1.2031	1.8000	2.7234	3.6661
500	1.2066	1.8005	2.7235	3.6661
864	1.2082	1.8007	2.7235	3.6661
1372	1.2089	1.8007	2.7235	3.6661
2048	1.2093	1.8007	2.7235	3.6661
2916	1.2096	1.8008	2.7235	3.6661
4000	1.2097	1.8008	2.7235	3.6661
∞	1.2102	1.8008	2.7235	3.6661

B. Reduced inverse second moment of the frequency distribution. $\langle[\nu(\text{Einstein})/\nu]^2\rangle$ is tabulated for periodic face-centered crystals. The $n=\infty$ column corresponds to the nearest-neighbor case treated in Ref. 14. The moments for infinite crystals are extrapolations based on a number dependence of order $N^{-1/3}$. As a further check of our extrapolations we calculated the frequencies for 16 384 Maxwellian particles. The reduced Einstein frequency, 1.21006, the reduced inverse second moment, 2.55028, and the reduced free energy, 0.51246, agree with our extrapolations from the smaller crystals.

N	$n=4$	$n=6$	$n=9$	$n=12$	$n=\infty$
4	1.1250	0.9722	0.9101	0.8861	0.8333
32	3.0020	1.7494	1.4861	1.3964	1.2204
108	2.4471	1.8542	1.6563	1.5671	1.3614
256	2.4391	1.9614	1.7606	1.6635	1.4377
500	2.4526	2.0320	1.8255	1.7233	1.4848
864	2.4678	2.0803	1.8691	1.7636	1.5167
1372	2.4817	2.1152	1.9004	1.7925	1.5397
2048	2.4939	2.1413	1.9240	1.8143	1.5570
2916	2.5045	2.1617	1.9423	1.8313	1.5705
4000	2.5138	2.1780	1.9569	1.8449	1.5813
∞	2.631	2.322	2.088	1.968	1.679

C. Free energy of the Einstein model relative to that calculated from lattice dynamics. $C(N)$ is tabulated for face-centered periodic crystals. The results for the inverse 12th power potential are taken from Ref. 16. Extrapolations to get $C(\infty)$ are based on a $C(N)$ number dependence of order $\ln N/N$, as described in Ref. 14. Additional terms of order N^{-1} and, for $n=4$ and 6, $N^{-4/3}$ were used in making the estimates.

N	$n=4$	$n=6$	$n=9$	$n=12$	$n=\infty$
4	−0.06371	−0.16094	−0.20395	−0.22108	−0.25993
32	+0.63710	+0.35112	+0.25010	+0.20970	+0.11871
108	0.52221	0.39124	0.32311	0.28850	0.19713
256	0.51338	0.41336	0.34912	0.31464	0.22247
500	0.51186	0.42335	0.36002	0.32553	0.23304
864	0.51166	0.42840	0.36536	0.33088	0.23824
1372	0.51175	0.43122	0.36830	0.33381	0.24111
2048	0.51189	0.43291	0.37006	0.33557	0.24282
2916	0.51201	0.43399	0.37117	0.33668	0.24391
4000	0.51212	0.43472	0.37191	0.33743	0.24464
∞	0.51266	0.43696	0.37420	0.33972	0.24689

correlated with several *different* microscopic quantities. The melting transition scales accurately with the inverse second moment $\langle \nu^{-2} \rangle$ (Lindemann) of the frequency distribution or with the free volume (Ross). The thermal energy of the *fluid* scales accurately with the solidlike Einstein frequency. These correlations carry over fairly well to the extremely soft one-component Coulomb system studied by Brush, Sahlin, and Teller. In practice, the universal equation of state suggested by Fig. 5 should prove to be a useful approximation.

A derivation explaining this energy-temperature equation of state from a *simple* theoretical model would be satisfying.

Two problems of somewhat academic interest are suggested by this study. First, what is the best analog of Lindemann's melting rule for two-dimensional systems? Second, what are the fusion properties for the limiting $1/r^3$ potential? It seems likely that the third power case is more amenable to an exact theoretical treatment than the other powers.

For all inverse power potentials there is a striking similarity between the fluid and single-occupancy solid properties. It seems likely, based on these results, that the physical idea underlying Lennard-Jones and Devonshire's theory of melting[35] is basically sound. An investigation of the properties of a system in which particles are randomly distributed over $2N$ cells would probably show that this system mimics a fluid very well.

ACKNOWLEDGMENTS

It is a pleasure to thank Warren G. Cunningham once again for carrying out the major part of the computer calculations and Roger McLain for drawing the figures. Richard Grover's interest has been of great help too. He pointed out the similarity of our inverse power thermodynamics to those of Ref. 29 and provided, through his work on the scaling of liquid-metal equations of state, stimulus for correlating our results.

* Work performed under the auspices of the U.S. Atomic Energy Commission.

[1] See the series of papers by V. Magnasco, G. F. Musso, and R. McWeeny, J. Chem. Phys. **46,** 4015; **47,** 1723, 4617, and 4629 (1967).

[2] H. F. Schaefer III, D. R. McLaughlin, F. E. Harris, and B. J. Alder, Phys. Rev. Letters **25,** 988 (1970).

[3] The most advanced work with realistic forces between molecules has been carried out by Barker and co-workers. See M. V. Bobetic and J. A. Barker, Phys. Rev. B **2,** 4169 (1970) and J. A. Barker, M. L. Klein, and M. V. Bobetic, *ibid.* B **2,** 4176 (1970).

[4] W. W. Wood and J. D. Jacobson, J. Chem. Phys. **27,** 1207 (1957); B. J. Alder and T. E. Wainwright, J. Chem. Phys. **27,** 1208 (1957).

[5] B. J. Alder, W. G. Hoover, and D. A. Young, J. Chem. Phys. **49,** 3688 (1968).

[6] Boltzmann devoted a chapter of his gas-theory lectures to the dynamics of Maxwellian particles. See *Lectures on Gas Theory,* translated by S. G. Brush (University of California Press, Berkeley, Calif., 1964).

[7] C. Domb, Phil. Mag. **42,** 1316 (1951).

[8] W. L. McMillan, Phys. Rev. **138A,** 442 (1965).

[9] J.-P. Hansen and D. Levesque, Phys. Rev. **165,** 293 (1968).

[10] N. A. Metropolis, A. W. and M. N. Rosenbluth, A. H. and E. Teller, J. Chem. Phys. **21,** 1087 (1953).

[11] For a recent comprehensive review see W. W. Wood in *The Physics of Simple Liquids,* edited by H. N. V. Temperley, J. S. Rowlinson, and G. S. Rushbrooke (North-Holland, Amsterdam, 1968), Chap. 5.

[12] A classical phase diagram for a realistic potential (Lennard-Jones) was worked out by J.-P. Hansen and L. Verlet, Phys. Rev. **184,** 151 (1969). For quantum effects see J.-P. Hansen and J.-J. Weis, Phys. Rev. **188,** 314 (1969).

[13] I. Oppenheim and P. Mazur, Physica **23,** 197 (1957); W. G. Hoover and B. J. Alder, J. Chem. Phys. **46,** 686 (1967).

[14] W. G. Hoover, J. Chem. Phys. **49,** 1981 (1968).

[15] B. R. A. Nijboer and F. W. De Wette, Physica **23,** 309 (1957).

[16] W. G. Hoover, M. Ross, K. W. Johnson, D. Henderson, J. A. Barker, and B. C. Brown, J. Chem. Phys. **52,** 4931 (1970).

[17] J.-P. Hansen, Phys. Rev. A **2,** 221 (1970).

[18] M. Born and K. Huang, *Dynamical Theory of Crystal Lattices* (Oxford U. P., London, 1954).

[19] A. C. Holt, W. G. Hoover, S. G. Gray, and D. R. Shortle, Physica **49,** 61 (1970).

[20] See Frenkel's discussion of the significance of the divergence in *Kinetic Theory of Liquids* (Dover, New York, 1955), pp. 124–125.

[21] For a recent correlation of face-centered and body-centered metal melting data see J. N. Shapiro, Phys. Rev. B **1,** 3982 (1970).

[22] F. H. Ree, J. Chem. Phys. **53,** 920 (1970).

[23] A. A. Maradudin, E. W. Montroll, and G. H. Weiss, Solid State Phys. Suppl. **3** (1963), Sec. VII.2.

[24] Anharmonic effects on the mean-squared displacement are estimated by V. V. Goldman, Phys. Rev. **174,** 1041 (1968). He estimates a decrease of about 20% in the Lindemann fraction for argon at the melting point due to anharmonic terms.

[25] David A. Young (private communication).

[26] M. Ross, Phys. Rev. **184,** 233 (1969). Ross' melting rule is successfully applied to a wider class of experimental and computer data in a melting theory review to be published in Contemporary Physics.

[27] See Refs. 7, 26, and W. G. Hoover and M. Ross, "Statistical Theories of Melting," Comtemporary Phys. (to be published).

[28] W. G. Hoover and F. H. Ree, J. Chem. Phys. **49,** 3609 (1968).

[29] S. G. Brush, H. L. Sahlin, and E. Teller, J. Chem. Phys. **45,** 2102 (1966).

[30] For cubic crystals the Einstein frequency is given by $(2\pi\nu_{\text{Einstein}})^2 = (3m)^{-1}\Sigma\phi'' + 2\phi'/r$, where the sum is over the fixed neighbors of the oscillating particle.

[31] By a "Grüneisen" theory we mean the relation $P_{\text{thermal}} \equiv \gamma E_{\text{thermal}}/V$, where γ is the logarithmic derivative of a suitably defined frequency, $\gamma \equiv -d\ln\theta/d\ln V$. For inverse power potentials *all* of the normal-mode frequencies are proportional to $V^{-(n+2)/6}$ and γ is $(n+2)/6$. For other potentials an average γ has to be used.

[32] J. E. Mayer and M. G. Mayer, *Statistical Mechanics* (Wiley, New York, 1940).

[33] G. A. Mansoori and F. B. Canfield, J. Chem. Phys. **51,** 4958 (1969); the same theory was developed independently by J. Rasaiah and G. Stell, Mol. Phys. **18,** 249 (1970). Similar perturbation theories have been introduced and studied by J. A. Barker and D. Henderson, J. Chem. Phys. **47,** 2856; 4714 (1967); Phys. Rev. A **1,** 1266 (1970).

[34] M. L. Klein, G. K. Horton, and J. L. Feldman, Phys. Rev. **184,** 968 (1969).

[35] J. E. Lennard-Jones and A. F. Devonshire, Proc. Roy. Soc. (London) **A169,** 317 (1939).